Surfaces and Interfaces 9 (2017) 1–8

Contents lists available at ScienceDirect

Surfaces and Interfaces

journal homepage: www.elsevier.com/locate/surfin

Aluminium oxide-silica/carbon composites from rice husk as a bi-functional heterogeneous catalyst for the one-pot sequential reaction in the conversion of glucose

Syed M. Al-Amsyar, Farook Adam*, Eng-Poh Ng

School of Chemical Sciences, Universiti Sains Malaysia, 11800 Penang, Malaysia

ARTICLE INFO

Keywords:
Rice husk
Aluminium silica/carbon composite
Heterogeneous catalysis
Glucose conversion
Bifunctional acid catalyst

ABSTRACT

A simple preparation of aluminium oxide-grafted silica/carbon composites (Al-SiO_2/C) from rice husk is reported. This composite has been employed as a bifunctional heterogeneous Lewis-Brønsted acid catalyst in the conversion of glucose into 5-hydroxymethylfurfural (HMF). SEM images showed the presence of bulk and nanosized Al-SiO_2/C particles which were closely packed on the catalyst's surface. XPS data proved the presence of Al in the form of aluminium oxide and graphitic carbon with several functional groups. The XRD data confirmed this catalyst was amorphous. The results from N_2 adsorption-desorption isotherm showed Al grafting did not affect its physicochemical properties. Pyridine-probe FTIR verified the existence of Lewis and Brønsted acid sites. A yield of 52% 5-hydroxymethylfurfural (HMF) was obtained at 170 °C in N-methylpyrrolidone (NMP) solvent. The catalyst proved to be stable without significant loss of yield after several recycling experiments.

1. Introduction

The development of catalyst from waste material is gaining prominence due to economic and environmental concern. There are several approaches currently being pursued for the utilization of waste material in catalytic activity. For instance, the waste material are directly used as active materials, as catalysts precursor, as surface-modified materials, and as pre-catalyst [1]. One of the most abundant agricultural wastes is rice husk, produced from the rice milling industry. It consists of lignocellulosic components such as cellulose, hemicelluloses, lignin, and also silica [2].

Basically, silicic acid and water are taken into the plant via the roots from the soil. The growing paddy plant deposits the silicic acid as silica on the rice husks cell wall, on the surface of leaves and stems in the form of silica-cuticle and silica-cellulose double layers. In addition, small and large silica particles exist in the intercellular layers [3,4]. Reports on the utilization of rice husk as silica and carbon source is abundant in literature [5–7].

For example, utilizing silica from rice husk as a catalyst precursor have been demonstrated recently via grafting and sol-gel techniques. Furthermore, addition of surfactant will create pores in the solid structure. Such treatment can increase the surface area of the prepared catalyst. These materials showed good potential as heterogeneous catalysts such as in alkylation, benzylation, degradation of phenol, oxidation, and esterification [8]. Lignocellulosic components in rice husk can be transformed into carbon material by carbonization under air or N_2 atmosphere. Recently, silica in rice husk has been used as a natural template to synthesize hierarchical porous carbon [9].

However, the direct preparation and use of rice husk as silica/carbon composite is scarcely reported. Due to its hybrid organic-inorganic nature, the silica/carbon composite can be advantageously utilized, especially as heterogeneous catalyst in organic synthesis [10], transparent conductors [11], and solar absorber [12]. The presence of silica can provide durability and thermal stability for heterogeneous catalyst. Besides, the carbon from the lignocellulosic components will have weak Brønsted acid sites which is crucial in some organic reactions [13].

In this era of diminishing petroleum reserves, researchers around the world have made tremendous efforts to reduce the dependency on crude oil by shifting their focus to use biomass as a chemical feedstock [14]. 5-hydroxymethylfurfural (HMF) has been identified as a potential chemical intermediate in biofuel and fine chemicals [15]. The rehydration of HMF will produce levulinic acid (LA), a highly potential feedstock for herbicide, polymers, and petrochemical production [16].

HMF can be obtained from the dehydration of C6 sugars such as glucose and fructose in which the latter is a more reactive substrate. The glucose enolyzes very slowly and the enolization is a rate determining step for the formation of HMF from glucose [17]. The

* Corresponding author.
E-mail addresses: farook@usm.my, farookdr@gmail.com (F. Adam).

http://dx.doi.org/10.1016/j.surfin.2017.06.011
Received 20 January 2017; Received in revised form 15 June 2017; Accepted 22 June 2017
Available online 04 July 2017

intricacy to obtain high selectivity and isolated yields render HMF to become costly and thus restrict its potential as a key chemical platform. However, the use of glucose as a substrate is more attractive due to its lower cost than fructose [18].

The conversion of glucose into fructose involves isomerization aided by Lewis acid on the catalyst. This is followed by dehydration into HMF in the presence of Brønsted acid [19]. Some researchers have reported the utilization of solid acid catalyst to produce HMF from sugar. Zeolite-Y has been tested as heterogeneous catalyst in aqueous glucose solutions [20]. Although quantitative glucose conversion was achieved, but only less than 10% of HMF yield was attained. The presence of levulinic acid, formic acid, and coke deposition were also detected as by-products. Niobic acid, $Nb_2O_5.nH_2O$, a heterogeneous Lewis acid catalyst has been tested in glucose conversion into HMF in water [21]. The NbO_4 tetrahedral Lewis acid sites on the surface immediately form $NbO_4{-}H_2O$ adducts in the presence of water. A yield of 12.1% HMF was obtained. However, $Na^+/Nb_2O_5.nH_2O$ without Brønsted acid sites showed a similar yield (12.4%). This indicates the formation of HMF under this catalytic system was catalyzed by Lewis acid site alone.

In order to obtain high conversion and high HMF yield, the use of organic solvents instead of water has been reported. This step could prevent the rehydration process thus eliminating the formation of levulinic acid. The combination of hydrotalcite and Amberlyst-15 as bifunctional acid-base catalyst has been employed in converting glucose into anhydroglucose (levoglucosan) or HMF [22]. Amberlyst-15 was able to dehydrate glucose into anhydroglucose (32%) in a polar aprotic solvents at 100 °C within 3 hours. However, anhydroglucose could not be dehydrated into HMF. The presence of hydrotalcite allowed isomerization of glucose into fructose. Amberlyst-15 was then able to dehydrate fructose into HMF. The highest yield of HMF in this catalytic system was 41% with 72% glucose conversion in DMF solvent. By adding a small amount of water, HMF selectivity increased to 57–64%.

HMF selectivies of over 70% were achieved from glucose using Sn-Beta catalyst and HCl in a biphasic system [23]. In the aqueous phase, isomerization of glucose and dehydration of fructose took place. After that, the HMF will be extracted into the organic phase from the aqueous phase. The addition of inorganic salts have proved to improve HMF partitioning into the organic phase thus, suppressing the undesired-side reactions [24]. The efficiency of the biphasic system also has been reported [25]. They employed Sn-montmorilonite as a bifunctional Lewis-Brønsted acid catalysts by using similar biphasic solvents (THF/H_2O/NaCl). A yield of 59.3% HMF was reported at 160 °C in 3 hours. The addition of HCl was not necessary since Sn-montmorilonite consists of Lewis acid sites for isomerization and Brønsted acid sites for dehydration.

Herein, a facile method is reported for preparing silica/carbon composites directly from the rice husk. This was followed by grafting with aluminium oxide to act as a bifunctional Lewis-Brønsted acid catalyst in converting glucose into HMF.

2. Materials and methods

2.1. Preparation of the catalyst

The pre-treatment of rice husk (RH) has been described previously [8,26]. The RH was carbonized in a muffle furnace. First the RH was placed in a stainless steel boat and placed inside the muffle furnace. The sample was heated from room temperature (30 °C) to reach the desired carbonization temperature of 400 °C at a heating rate of 5 °C/minute under air atmosphere. The desired carbonization temperature was maintained for another 1 h. This procedure will transform lignocellulosic components in rice husk into graphitic carbon. The resulting sample was labeled as SiO_2/C-x, where x = 400 (carbonization temperature). Other samples were prepared for x = 350, 450, and 500.

For Al grafting, 0.05 g of aluminium trichloride hexahydrate ($AlCl_3.6H_2O$) was dissolved in 3.0 mL of methanol. A mass of 0.5 g of the SiO_2/C-400 was added to the solution and stirred for an hour. The solid was filtered and dried in an oven at 50 °C overnight. Then, the sample was calcined by heating the composite in a muffle furnace under air atmosphere (furnace temperature = 300 °C, duration = 6 h). This process will produce aluminium oxide-grafted silica/carbon, denoted as Al-SiO_2/C-400. Similarly Al-SiO_2/C-350, Al-SiO_2/C-450, and Al-SiO_2/C-500 were prepared.

2.2. Characterization of the catalyst

The morphology of the catalysts were studied using scanning electron microscopy (SEM, FEI model Quanta FEG 650 with an electron beam resolution of 3.0 nm at 10.0 kV). The elemental mapping was carried out by using EDX which was coupled with SEM (X-Max 50 mm^2 SDD detectors with a resolution of 127 nm at MnK_α). The distance between sample and pole piece was 10 mm. The local structure of Al-SiO_2/C-400 was detailed by using X-ray Photoelectron Spectroscopy (XPS), using High Resolution Multi Technique X-ray Spectrometer (Axis Ultra DLD XPS, Kratos).

The surface area and porosity of the catalysts were analyzed by using N_2 adsorption–desorption analysis (Micromeritics ASAP 2020 porosimeter). The samples were initially degassed at 110 °C for 8 h under vacuum prior to being analyzed. The structural information of the catalysts were characterized by powder X-ray Diffraction (Siemens Diffractometer D5000 Kristalloflex, equipped with Cu K_α radiation, $\lambda = 0.154$ nm) with a step size of 0.05° from 10 to 90° (high angle). The voltage supplied was 40 kV with a current of 30 mA.

Pyridine-probe FTIR spectra were recorded using a Nicolet 6700 FT-IR spectrometer. Prior to measurement, the samples were ground and pressed to obtain a wafer (area 2 cm^2, mass of 11–13 mg) before being introduced into the vacuum IR cell. The samples were then pre-activated under vacuum (10^{-6} mbar) at 200 °C for 1.5 h. The reference spectrum was first recorded after cooling and then pyridine was introduced to the samples at 25 °C for 30 s. The samples were evacuated at 50 °C to desorb pyridine and the spectra were recorded with a resolution of 4 cm^{-1} and 128 scans accumulation. The thermal properties of the composite were determined by thermogravimetric analysis (TGA) performed using a TGA SDTA851e instrument operating from 30 to 920 °C at 10 °C min^{-1} under oxygen atmosphere.

2.3. Catalytic reactions

The catalytic testing was carried out by placing the catalyst, substrate, internal standard (biphenyl), and solvent in the Ace pressure tube (Sigma-Aldrich). The reaction mixture was stirred at 700 rpm for a desired time and temperature by using a pre-heated silicone oil bath coupled with temperature sensor. Next, the reaction mixture was filtered before deuterated DMSO solvent was added to the filtrate for NMR analysis. Subsequent calculations and product identification were carried out. For catalyst reuse experiment, the reaction mixture was separated by centrifugation and the supernatant was removed. The catalyst was washed with acetone several times and dried in oven at 100 °C. It was ground to powder before being used in subsequent reactions.

3. Results and discussion

3.1. Catalyst characterization

3.1.1. Scanning electron microscope (SEM) – energy dispersive X-ray (EDX) analysis

The SEM images showed bulk Al-SiO_2/C-400 (Fig. 1a) and closely-packed Al-SiO_2/C-400 particles spotted on the surface of the cell (Fig. 1b). Further enlargement of this image revealed that the size of closely-packed Al-SiO_2/C-400 particles was less than 100 nm (Fig. 1c) with EDX analysis confirming the presence of Al, Si, O, and C atoms (Fig. 1d).

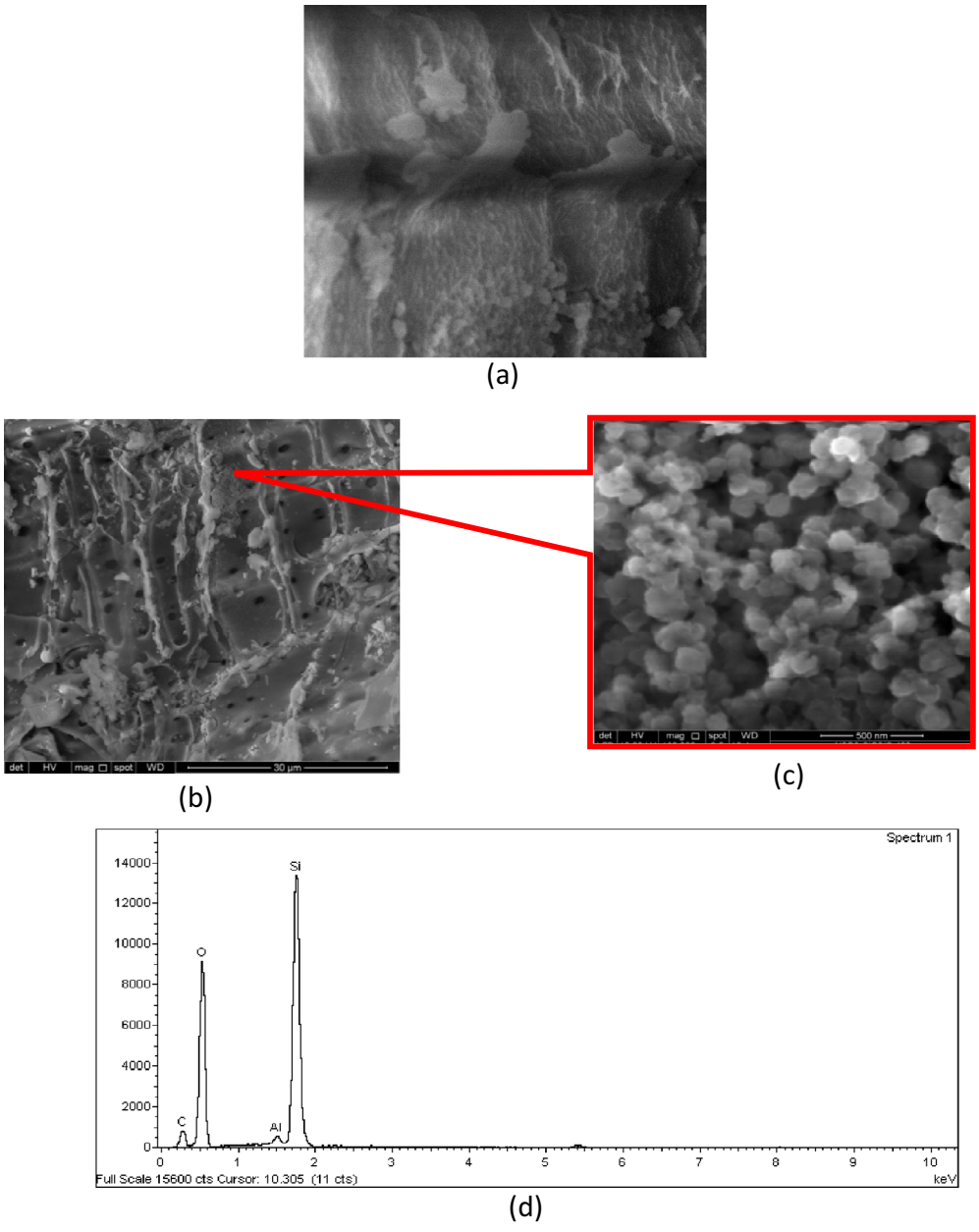

Fig. 1. SEM image of (a) bulk Al-SiO_2/C-400 at 100k magnification (b) nanosized Al- SiO_2/C-400 at 5k magnification and (c) further enlargement of its nanoparticles at 160k magnification (d) The EDX analysis of nanosized Al-SiO_2/C-400 catalyst particles.

3.1.2. X-ray diffraction (XRD) analysis and elemental mapping

The Al-SiO_2/C-400 composite retained its amorphous structure after Al grafting, as corroborated by XRD. It exhibited two broad and weak peaks around 23° and 45° which correspond to the graphitic ([002] and [101] or [100]) planes, respectively (Fig. 2) [9]. However, the diffraction peak of amorphous silica at 23° was very strong and broad, and overlapped with graphitic [002] diffraction band [27]. The absence of crystalline aluminium oxide peaks indicated the Al_2O_3 particles were too small to be detected. It is thus presumed that these aluminium oxide particles were well-dispersed in silica/carbon matrix, thus preventing the aggregation of Al_2O_3 from forming a crystalline phase. In addition, the elemental mappings provide evidence that Al, Si, C, and O atoms were homogeneously dispersed in the catalyst framework (Fig. 3).

3.1.3. N_2 sorption analysis

N_2 sorption analysis demonstrated that the grafting of aluminium oxide had minimal effect on the porosity and morphology on the parent silica/carbon composite (Table 1). Both sample show Type IV isotherm with Type H3 hysteresis loop, indicating the presence of mesopore in

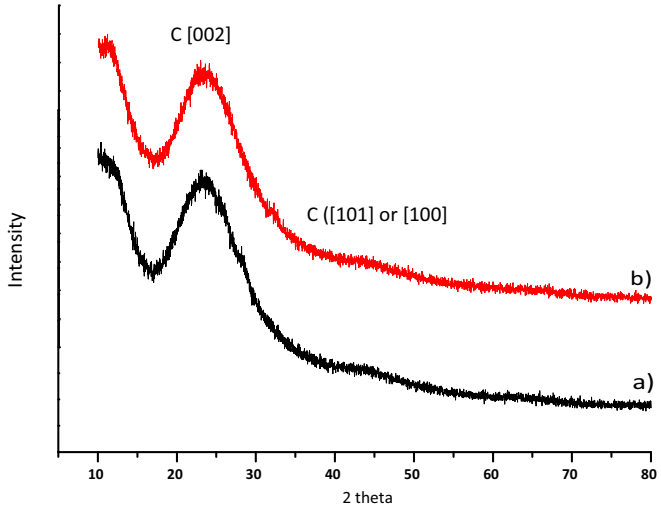

Fig. 2. The XRD pattern for SiO_2/C-400 composite a) before and b) after Al grafting.

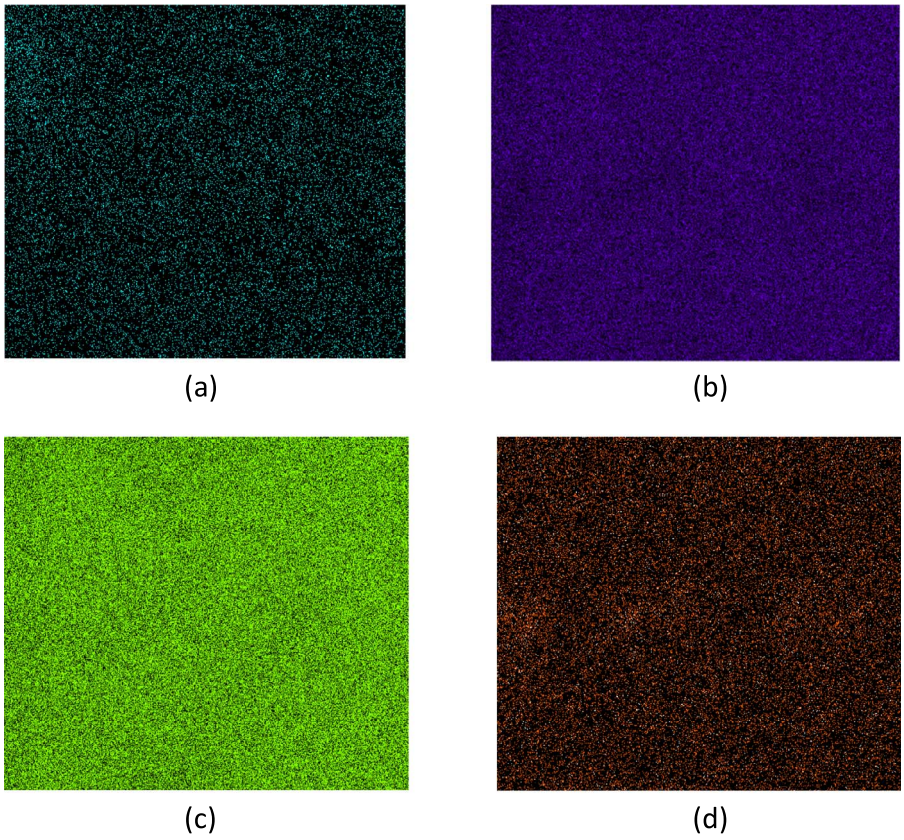

Fig. 3. Elemental mapping of (a) Al (b) Si (c) O (d) C atoms of bulk Al-SiO_2/C-400 at a 100k magnification (see Fig. 1a).

Table 1
The summary of textural data of SiO_2/C-400 catalyst before and after Al grafting.

Sample	S_{BET}[a] (m^2g^{-1})	V_{micro}[b] (cm^3g^{-1})	V_{total}[c] (cm^3g^{-1})	Pore width[d] (Å)
SiO_2/C-400	179	0.015	0.124	41
Al-SiO_2/C-400	141	0.013	0.100	45

[a] Calculated from the Brunauer–Emmett–Teller (BET) isotherm method.
[b] Calculated from t-plot method.
[c] Calculated from the Barret-Joyner Halenda (BJH) desorption cumulative volume of pores.
[d] Calculated from the Barret-Joyner Halenda (BJH) desorption average pore width.

their structure. Low pressure hysteresis (LPH) was also observed before and after grafting which was caused by unusual slow gas uptake. This phenomenon is common for porous solids with narrow pore opening, due to inappropriate outgassing and/or lack of equilibrium in the adsorption isotherm within the experimental time scale [28,29] (Fig. S1). Slight reduction of surface area (from 179 to 141 m^2g^{-1}) and total pore volume (from 0.124 to 0.100 cm^3g^{-1}) was detected when aluminium oxide was incorporated. However, the pore width increased slightly (from 41 to 45 Å) after the Al grafting, but this increase is minimal. Multimodal with narrow and broad pore size distribution of 40—45 nm became noticeable after Al grafting (Fig. S2).

3.1.4. Pyridine-probe FTIR

Lewis acidity was observed after the Al grafting (1610 and 1448 cm^{-1}), as confirmed by pyridine-probe FTIR (Fig. 4). The sample also showed the Brønsted acid site even before the introduction of Al (1560 and 1488 cm^{-1}) and it became more apparent after grafting (1640 cm^{-1}). Thus, Al-SiO_2/C-400 was shown to have dual functionalities of Lewis and Brønsted acid sites.

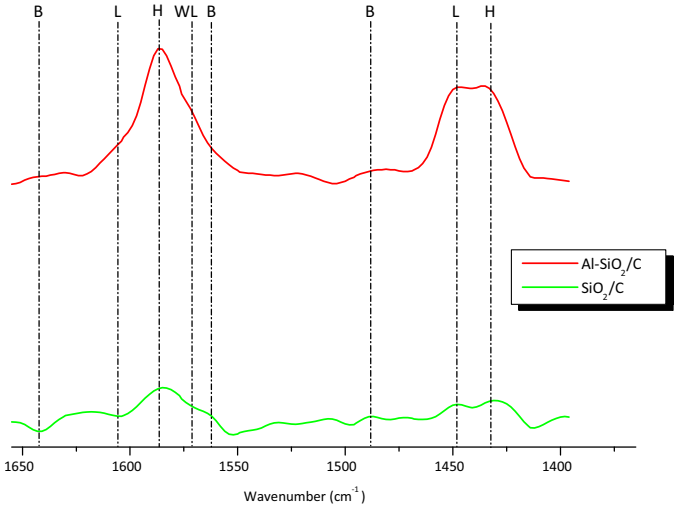

Fig. 4. FTIR after pyridine sorption and evacuation of SiO_2/C-400 and Al-SiO_2/C-400 at 25 °C. Hydrogen-bound pyridine (H), Brønsted acid (B), Lewis acid (L), weak Lewis acid (WL).

3.1.5. X-ray Photoelectron Spectroscopy (XPS)

The local structure of Al-SiO_2/C-400 was detailed by using X-ray Photoelectron Spectroscopy (XPS) (Fig. S3). The existence of elements such as Al, Si, O, N,and C was detected. The presence of N atoms were most probably due to the pre-treatment step of rice husk with HNO_3. The presence of Al—O bond for aluminium oxide was detected at 75.200 eV and neither Al—Al nor Al—C bonds were found (Fig. S4) [30]. The quantitative analysis showed 1.03 wt.% of Al which is close to the theoretical value (1.11 wt.%) as no Al content was expected to be lost during catalyst preparation.

Meanwhile, the deconvolution of carbon 1 s reveals that the lignocellulosic component was transformed into graphitic carbon with

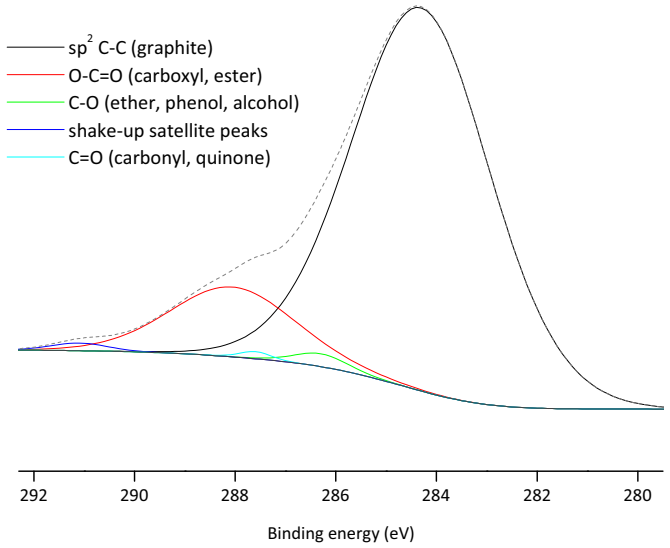

Fig. 5. The XPS spectra of C 1 s after deconvolution.

some functional groups such as carbonyl, carboxyl, and phenolic (Fig. 5) [31]. No C—Si bond was observed at 283.1 eV, thus ruling out the formation of silicon carbide composite during the carbonization process [32]. It indicates that Al oxide, silica, and graphitic carbon are evenly distributed in the catalyst framework without any chemical bonds involved with each other.

3.1.6. FTIR spectra analysis

FTIR spectra reveals that the graphitic carbon with —COOH functional groups became less significant at higher carbonization temperature (350, 400, and 450 °C) (Fig. 6, i-iii). The disappearance of the graphitic carbon with —COOH functional group was observable when it was carbonized at 500 °C (Fig. 6, iv). Thus, the catalyst was assigned as Al-SiO_2 instead of Al-SiO_2/C-500.

3.1.7. Thermogravimetric analysis (TGA)

From TGA, in all samples, the weight loss around 120 °C was due to the removal of physisorbed water. For Al-SiO_2/C-400, the weight percent of carbon and SiO_2 were 34.295% and 54.660%, respectively. However, decreasing carbonization temperature to 350 °C had increased the carbon content to 47.931% and decreased the SiO_2 content

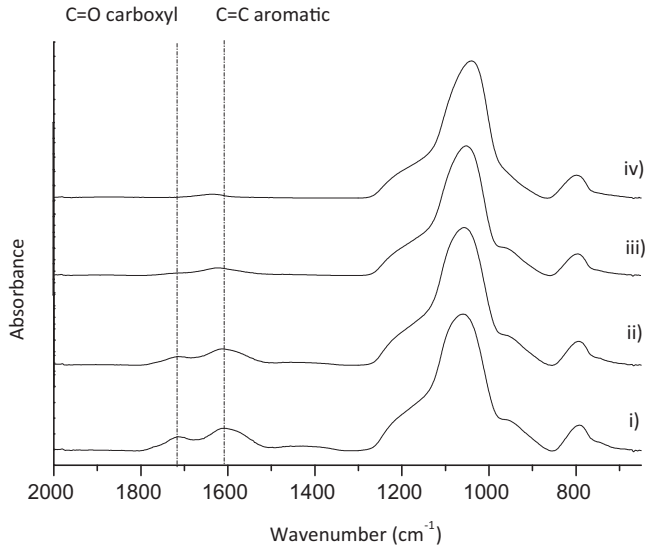

Fig. 6. FTIR spectra for Al-SiO_2/C-x at a different carbonization temperature (i) x = 350 °C; (ii) x = 400 °C; (iii) x = 450 °C; and (iv) x = 500 °C.

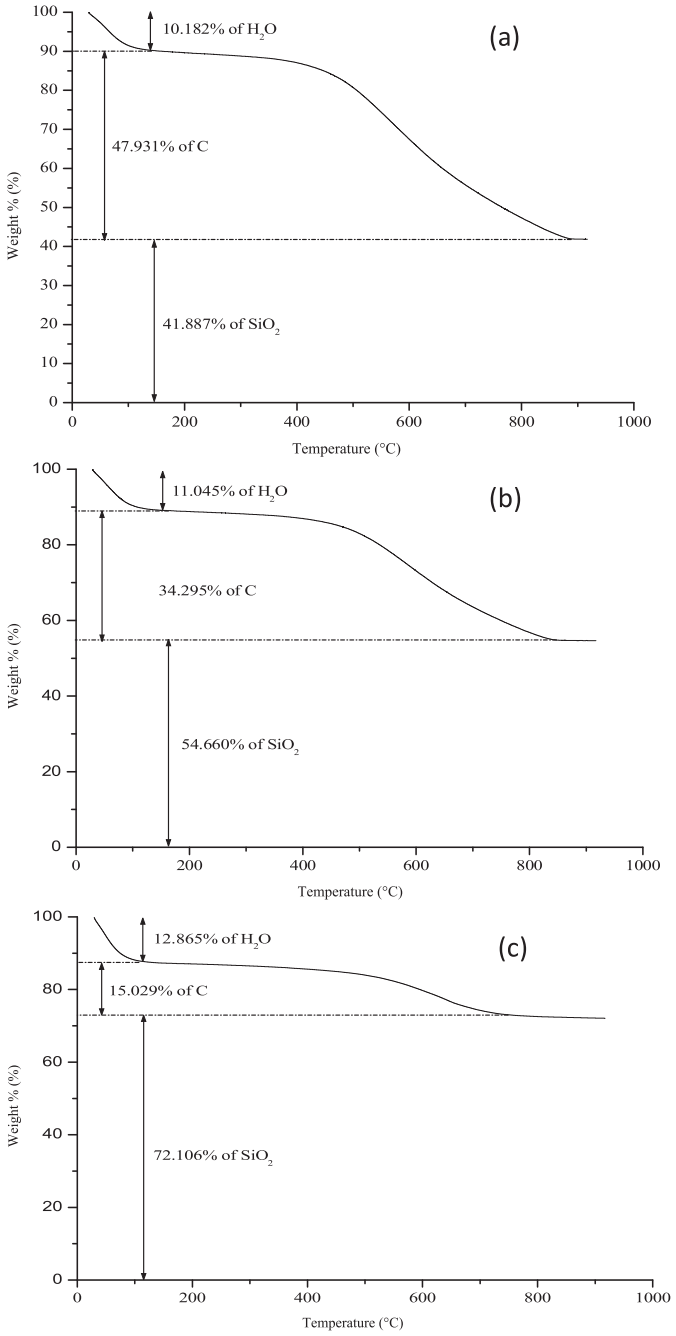

Fig. 7. TGA thermograms of (a) Al-SiO_2/C-350 (b) Al-SiO_2/C-400 (a) Al-SiO_2/C-450 catalysts.

to 41.887%. Whereas, increasing the carbonization temperature to 450 °C had decreased the carbon content to 15.029% and increased SiO_2 content to 72.106% (Fig. 7). Thus, carbon and SiO_2 content can be easily manipulated by changing the carbonization temperature.

3.2. Catalytic reactions

3.2.1. The screening of the catalysts

The catalyst screening for the conversion of glucose into HMF is shown in Fig. 8. The absence of catalyst resulted in ineffective conversion with only 2% of HMF detected. In addition, using the parent SiO_2/C-400 composite gave a similar yield. However, by introducing aluminium oxide onto the SiO_2/C-400 composite, 52% yield of HMF was obtained. This suggests the role of Al as Lewis acid site to isomerize glucose into fructose. This is followed by the dehydration step to

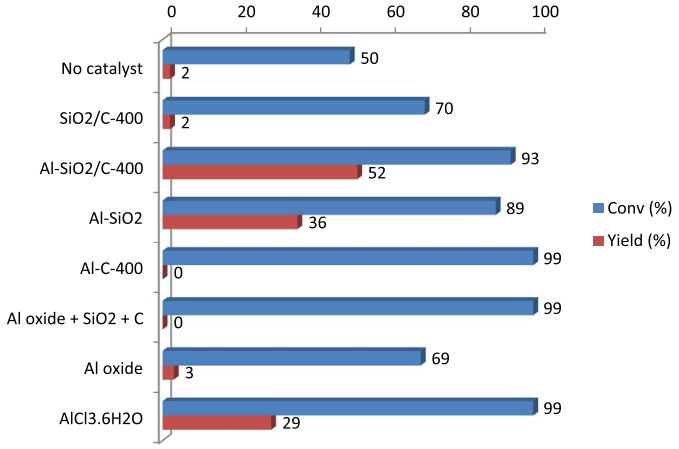

Fig. 8. Catalyst screening for the synthesis of HMF. Reaction condition: Catalyst 100 mg (0.0410 mmol of Al), glucose 1.0 mmol, NMP 4 mL, 170 °C, 5 h. Al oxide 0.0205 mmol. $AlCl_3.6H_2O$ 0.0410 mmol.

produce HMF, catalyzed by the Brønsted acid site from graphitic carbon and also silanol groups from silica. To support this assumption, Al-SiO_2 catalyst was tested in this reaction. As a result, a lower yield of HMF was obtained (36%). Therefore, it suggests that the graphitic carbon with–COOH functional group enhances dehydration of fructose to yield HMF.

Then, Al-C-400 catalyst was employed to see whether the presence of silica has any impact on this catalytic reaction. Surprisingly, no HMF was produced at all. It has been reported that silica plays an important role in promoting hydride transfer in the isomerization step of glucose [33]. Therefore, without the presence of silica, this isomerization is not possible. Al_2O_3 catalyst was also tested and only 3% of HMF was detected. An attempt to use $AlCl_3.6H_2O$ as a homogeneous catalyst produced only 29% yield. Interestingly, no HMF was observed when the physical mixture of aluminium oxide, silica, and carbon as a catalyst was tested. Elemental mapping confirmed that the homogeneity of this physically-mixed catalyst was lesser compared to Al-SiO_2/C-400 catalyst (Fig. S5).

To some extent, it indicates that under this catalyst system, the specific structure of Al-SiO_2/C-400 composite allows glucose to be converted into HMF smoothly. For that reason, the isomerization and dehydration steps could proceed continuously. In all cases, during the reaction, the color of the solution changed into dark brown, indicating the formation of humins [34]. It is assumed that humins originated from polymeric condensation of HMF and sugars [35].

Since the presence of carbon has been proved to enhance the yield of HMF, varying the carbon contents in the Al-SiO_2/C composite was carried out by changing the carbonization temperature of rice husk (350 °C and 450 °C). Consequently, using Al-SiO_2/C-450 as the catalyst had decreased the rate of HMF formation to 37 μmol h^{-1} while using Al-SiO_2/C-350 catalyst had decreased the rate to 32 μmol h^{-1} (Fig. 9). It means that in this catalyst system, the balance between silica and carbon fraction is very critical to obtain optimum yield since both are indispensable in promoting isomerization and dehydration steps. Thus, the carbonization temperature must be carefully selected to meet these two requirements. At some point, it can be assumed that the presence of −COOH groups which act as a weak Brønsted acid site can accelerate the rate of HMF formation.

3.2.2. Parameter study

The effect of Al loading onto silica/carbon composite on catalytic activity was investigated (Fig. 10a). The conversion and percentage yield of HMF decreased to 83% and 31%, respectively, when the amount of Al content was reduced to half. It is understood that the availability of Lewis acid site was less compared to the original condition. However, increasing the Al loading by two and four-fold gave

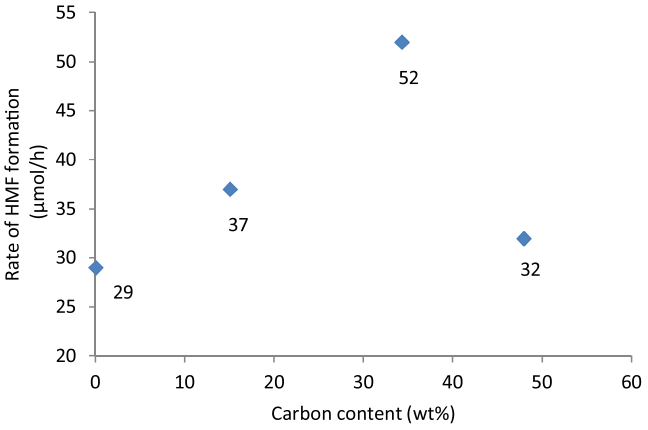

Fig. 9. The effect of varying carbon fraction on the rate of HMF production.

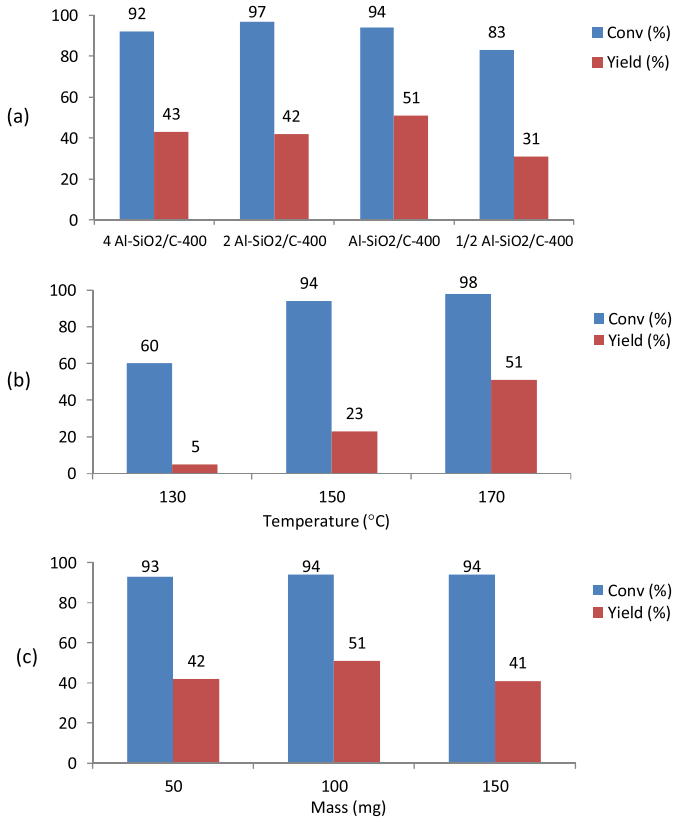

Fig. 10. (a) The effect of Al loading onto silica/carbon composite on catalytic activity of glucose conversion into HMF. Reaction condition: catalyst 100 mg, glucose 1.0 mmol, NMP 4 mL, 170 °C, 5 h. (b) The effect of reaction temperature on catalytic activity of glucose conversion into HMF. Reaction condition: Al-SiO_2/C-400 catalyst 100 mg, glucose 1.0 mmol, NMP 4 mL, 5 h. (c) The effect of catalyst dosage on catalytic activity of glucose conversion into HMF. Reaction condition: Al-SiO_2/C-400 catalyst, glucose 1.0 mmol, NMP 4 mL, 170 °C, 5 h.

lower yield. Possibly, the formation of undesired by-products was much faster under these conditions.

Reducing the reaction temperature from 170 °C to 150 °C had no significant effect on glucose conversion (Fig. 10b). However, HMF yield was reduced to 23%. It indicates that the rate of glucose conversion at 150 °C was similar to 170 °C. Nevertheless, the rate of HMF formation was decelerating. At 130 °C, both conversion and yield declined to 60% and 5% respectively. It suggests isomerization and dehydration steps are less pronounced at this temperature.

The effect of catalyst dosage is shown in Fig. 10c. The catalyst mass had no significant effect on glucose conversion. However, lower yield of

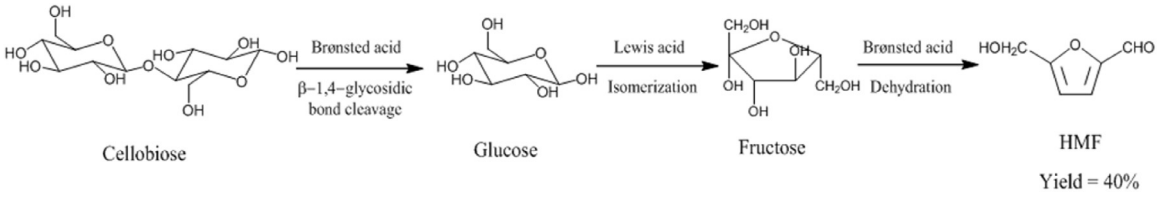

Fig. 11. Tandem glycosidic bond cleavage-isomerization-dehydration using Al-SiO_2/C-400 catalyst in one-pot reaction.

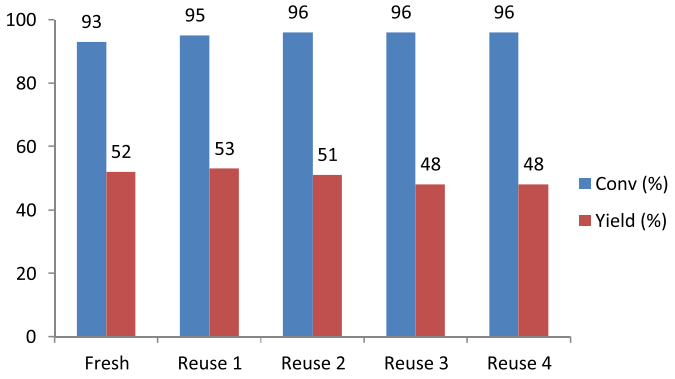

Fig. 12. Recycling experiments of Al-SiO_2/C-400 in glucose conversion.

HMF (42%) was obtained when 50 mg of catalyst was used, probably due to less active site in the reaction mixture. Surprisingly, only 41% of HMF yield was observed when 150 mg of catalyst was utilized, indicating the interphase mass transfer effect was occurred [36].

The applicability of this catalyst was tested in producing HMF from cellobiose, a disaccharide with two β-glucose linked with 1,4-glycosidic bond. This bond is much more stable than 1,4-α-glycosidic bond, which is found in maltose and starch. Therefore, the hydrolysis of 1,4-β-glycosidic bond is more difficult and require strong acids to cleave the bond. In this reaction, Al-SiO_2/C-400 was able to perform tandem glycosidic bond cleavage-isomerization-dehydration in a one-pot sequential reaction in which 40% yield of HMF was obtained (Fig. 11).

3.3. Recycling experiments

The result of reusability of this catalyst is shown in Fig. 12. No significant loss of HMF yield was observed after five cycles. This result proved the catalyst was stable and reusable. This was further confirmed by XRD (Fig. S6) and N_2 sorption analysis (Fig. S7) on the used catalyst. The structure remained intact despite the formation of aluminium oxalate which was identified from ICDD database. However, significant changes in its physicochemical properties (surface area, total pore volume, and pore width) were observed, as shown in Table S1. Nevertheless, these occurrences did not affect its catalytic performance in this reaction.

4. Conclusion

The design of silica/carbon-supported aluminium oxide was synthesized from rice husk. It was used as a heterogeneous catalyst in converting glucose into HMF. This demonstrates its dual role in the isomerization and dehydration reaction due to the existence of Lewis and Brønsted acid sites in the catalyst framework. Moreover, the unique composition and arrangements of nanoparticles and functionalized graphitic carbon enabled the conversion to be carried out in a one-pot reaction. This work showed some promising advantageous, such as: i) agricultural waste was used as silica/carbon precursor, ii) simple catalyst preparation method iii) low-cost reagents, and iv) good reusability.

Acknowledgements

The authors wish to thank Universiti Sains Malaysia and Ministry of Higher Education of Malaysia for awarding research grants (1001/PKIMIA/811269). Syed M. Al-Amsyar wishes to thank Universiti Malaysia Kelantan for the scholarship.

Supplementary materials

Supplementary material associated with this article can be found, in the online version, at http://dx.doi.org/10.1016/j.surfin.2017.06.011.

References

[1] M. Balakrishnan, V.S. Batra, J.S.J. Hargreaves, I.D. Pulford, Waste materials - catalytic opportunities: an overview of the application of large scale waste materials as resources for catalytic applications, Green Chem. 13 (2011) 16–24.
[2] L. Wang, X. Wang, B. Zou, X. Ma, Y. Qu, C. Rong, Y. Li, Y. Su, Z. Wang, Preparation of carbon black from rice husk by hydrolysis, carbonization and pyrolysis, Bioresour. Technol. 102 (2011) 8220–8224.
[3] H.A. Currie, C.C. Perry, Silica in plants: Biological, biochemical and chemical studies, Ann. Bot. 100 (2007) 1383–1389.
[4] J.F. Ma, K. Tamai, N. Yamaji, N. Mitani, S. Konishi, M. Katsuhara, M. Ishiguro, Y. Murata, M. Yano, A silicon transporter in rice, Nature 440 (2006) 688–691.
[5] F. Adam, A. Iqbal, The oxidation of styrene by chromium–silica heterogeneous catalyst prepared from rice husk, Chem. Eng. J. 160 (2010) 742–750.
[6] L. Muniandy, F. Adam, A.R. Mohamed, E.-P. Ng, N.R.A. Rahman, Carbon modified anatase TiO_2 for the rapid photo degradation of methylene blue: A comparative study, Surf. Interfaces 5 (2016) 19–29.
[7] M.S. Masoud, W.M. El-Saraf, A.M. Abdel-Halim, A.E. Ali, E.A. Mohamed, H.M.I. Hasan, Rice husk and activated carbon for waste water treatment of El-Mex Bay, Alexandria Coast, Egypt, Arab. J. Chem. (2012).
[8] F. Adam, J.N. Appaturi, A. Iqbal, The utilization of rice husk silica as a catalyst: Review and recent progress, Catal. Today. 190 (2012) 2–14.
[9] S. Tabata, H. Iida, T. Horie, S. Yamada, Hierarchical porous carbon from cell assemblies of rice husk for in vivo applications, Medchemcomm 1 (2010) 136–138.
[10] E. Sari, M. Kim, S.O. Salley, K.Y.S. Ng, A highly active nanocomposite silica-carbon supported palladium catalyst for decarboxylation of free fatty acids for green diesel production: Correlation of activity and catalyst properties, Appl. Catal. A Gen. 467 (2013) 261–269.
[11] S. Watcharotone, D.a. Dikin, S. Stankovich, R. Piner, I. Jung, G.H.B. Dommett, G. Evmenenko, S.E. Wu, S.F. Chen, C.P. Liu, S.T. Nguyen, Graphene- silica composite thin films as transparent conductors, Nano Lett 7 (2007) 1888–1892.
[12] Y. Mastai, S. Polarz, M. Antonietti, Silica–carbon nanocomposites—a new concept for the design of solar absorbers, Adv. Funct. Mater. 12 (2002) 197–202.
[13] P.W. Chung, A. Charmot, O.A. Olatunji-Ojo, K.A. Durkin, A. Katz, Hydrolysis catalysis of Miscanthus xylan to xylose using weak-acid surface sites, ACS Catal 4 (2014) 302–310.
[14] G.W. Huber, J.N. Chheda, C.J. Barrett, J.A Dumesic, Production of liquid alkanes by aqueous-phase processing of biomass-derived carbohydrates, Science 308 (2005) 1446–1450.
[15] J.N. Chheda, G.W. Huber, J.A. Dumesic, Liquid-phase catalytic processing of biomass-derived oxygenated hydrocarbons to fuels and chemicals, Angew. Chem. - Int. Ed. 46 (2007) 7164–7183.
[16] T. Werpy, G. Petersen, Top Value Added Chemicals from Biomass (No. DOE/GO-102004-1992), Pacific Northwest National Laboratory and National Renewable Energy Laboratory, Department Of Energy, Washington DC, 2004.
[17] M.J. Antal, W.S. Mok, G.N. Richards, Mechanism of formation of 5-(hydroxymethyl)-2-furaldehyde from D-fructose an sucrose, Carbohydr. Res. 199 (1990) 91–109.
[18] F.K. Kazi, A.D. Patel, J.C. Serrano-Ruiz, J.A. Dumesic, R.P. Anex, Techno-economic analysis of dimethylfuran (DMF) and hydroxymethylfurfural (HMF) production from pure fructose in catalytic processes, Chem. Eng. J. 169 (2011) 329–338.
[19] V. Choudhary, S.H. Mushrif, C. Ho, A. Anderko, V. Nikolakis, N.S. Marinkovic, A.I. Frenkel, S.I. Sandler, D.G. Vlachos, Insights into the interplay of lewis and brønsted acid catalysts in glucose and fructose conversion to 5-(Hydroxymethyl) furfural and levulinic acid in aqueous media, J. Am. Chem. Soc. 135 (2013) 3997–4006.
[20] K. Lourvanij, G. Rorrer, Reactions of aqueous glucose solutions over solid-acid Y-

zeolite catalyst at 100-160 °C, Ind. Eng. Chem. Res. 32 (1993) 11–19.
[21] K. Nakajima, Y. Baba, R. Noma, M. Kitano, J. Kondo, S. Hayashi, M. Hara, $Nb_2O_5 \cdot nH_2O$ as a heterogeneous catalyst with water-tolerant Lewis acid sites, J. Am. Chem. Soc. 133 (2011) 4224.
[22] M. Ohara, A. Takagaki, S. Nishimura, K. Ebitani, Syntheses of 5-hydroxymethylfurfural and levoglucosan by selective dehydration of glucose using solid acid and base catalysts, Appl. Catal. A Gen. 383 (2010) 149–155.
[23] E. Nikolla, Y. Román-Leshkov, M. Moliner, M.E. Davis, One-pot synthesis of 5-(hydroxymethyl)furfural from carbohydrates using tin-beta zeolite, ACS Catal 1 (2011) 408–410.
[24] Y. Román-Leshkov, C.J. Barrett, Z.Y. Liu, J.a. Dumesic, Production of dimethylfuran for liquid fuels from biomass-derived carbohydrates, Nature 447 (2007) 982–985.
[25] J. Wang, J. Ren, X. Liu, J. Xi, Q. Xia, Y. Zu, G. Lu, Y. Wang, Direct conversion of carbohydrates to 5-hydroxymethylfurfural using Sn-Mont catalyst, Green Chem. 14 (2012) 2506–2512.
[26] F. Adam, M.S. Batagarawa, Tetramethylguanidine-silica nanoparticles as an efficient and reusable catalyst for the synthesis of cyclic propylene carbonate from carbon dioxide and propylene oxide, Appl. Catal. A Gen. 454 (2013) 164–171.
[27] T.-H. Liou, Evolution of chemistry and morphology during the carbonization and combustion of rice husk, Carbon. 42 (2004) 785–794.
[28] A.M. Silvestre-Albero, J.M. Juárez-Galán, J. Silvestre-Albero, F. Rodríguez-Reinoso, Low-pressure hysteresis in adsorption: An artifact? J. Phys. Chem. C. 116 (2012).
[29] C. Reichenbach, D. Enke, J. Möllmer, D. Klank, M. Klauck, G. Kalies, Slow gas uptake and low pressure hysteresis on nanoporous glasses: The influence of equilibration time and particle size, Microporous Mesoporous Mater. 181 (2013) 68–73.
[30] J. van den Brand, P.C. Snijders, W.G. Sloof, H. Terryn, J.H.W. de Wit, J. Van Den Brand, J.H.W. De Wit, Acid-base characterization of aluminum oxide surfaces with XPS, J. Phys. Chem. B. 108 (2004) 6017–6024.
[31] S. Yumitori, Correlation of C1s chemical state intensities with the O1s intensity in the XPS analysis of anodically oxidized glass-like carbon samples, J. Mater. Sci. 35 (2000) 139–146.
[32] Y. Hijikata, H. Yaguchi, M. Yoshikawa, S. Yoshida, Composition analysis of SiO2/SiC interfaces by electron spectroscopic measurements using slope-shaped oxide films, 184 (2001) 161–166.
[33] N. Rai, S. Caratzoulas, D.G. Vlachos, Role of silanol group in Sn-beta zeolite for glucose isomerization and epimerization reactions, ACS Catal. 3 (2013) 2294–2298.
[34] J.B. Binder, R.T. Raines, Simple chemical transformation of lignocellulosic biomass into furans for fuels and chemicals, J. Am. Chem. Soc. 131 (2009) 1979–1985.
[35] R.J. Van Putten, J.C. Van Der Waal, E. De Jong, C.B. Rasrendra, H.J. Heeres, J.G. De Vries, Hydroxymethylfurfural, a versatile platform chemical made from renewable resources, Chem. Rev. 113 (2013) 1499–1597.
[36] R.J. Madon, M. Boudart, Experimental criterion for the absence of artifacts in the measurement of rates of heterogeneous catalytic reactions, Ind. Eng. Chem. Fundam. 21 (1982) 438–447.